PAPER

Free-electron laser with a plasma wave wiggler propagating through a magnetized plasma channel

IOP PUBLISHING LASER PHYSICS
Laser Phys. **23** (2013) 085005 (11pp) doi:10.1088/1054-660X/23/8/085005

Free-electron laser with a plasma wave wiggler propagating through a magnetized plasma channel

S Jafari[1], **F Jafarinia**[1] **and H Mehdian**[2]

[1] Department of Physics, University of Guilan, Rasht 41335-1914, Iran
[2] Department of Physics and Institute for Plasma Research, Tarbiat Moallem University, Tehran 15614, Iran

E-mail: SJafari@guilan.ac.ir

Received 11 April 2013, in final form 30 May 2013
Accepted for publication 31 May 2013
Published 4 July 2013
Online at stacks.iop.org/LP/23/085005

Abstract
A plasma eigenmode has been employed as a wiggler in a magnetized plasma channel for the generation of laser radiation in a free-electron laser. The short wavelength of the plasma wave allows a higher radiation frequency to be obtained than from conventional wiggler free-electron lasers. The plasma can significantly slow down the radiation mode, thereby relaxing the beam energy requirement considerably. In addition, it allows a beam current in excess of the vacuum current limit via charge neutralization. This configuration has a higher tunability by controlling the plasma density in addition to the γ-tunability of the standard FEL. The laser gain has been calculated and numerical computations of the electron trajectories and gain are presented. Four groups (I–IV) of electron orbits have been found. It has been shown that by increasing the cyclotron frequency, the gain for orbits of group I and group III increases, while a decrease in gain has been obtained for orbits of group II and group IV. Similarly, the effect of plasma density on gain has been exhibited. The results indicate that with increasing plasma density, the orbits of all groups shift to higher cyclotron frequencies. The effects of beam self-fields on gain have also been demonstrated. It has been found that in the presence of beam self-fields the sensitivity of the gain increases substantially in the vicinity of gyroresonance. Here, the gain enhancement and reduction are due to the paramagnetic and diamagnetic effects of the self-magnetic field, respectively.

(Some figures may appear in colour only in the online journal)

1. Introduction

Electron beam dynamics in plasma focusing channels has important applications in new plasma technologies, such as plasma lenses, plasma wakefield accelerators and novel coherent radiation sources [1–3]. The free-electron laser (FEL), as a high power radiation source, is a collective recoil lasing system in which particles scatter coherently the photons of the pump due to the wiggler field into a forward radiation mode [4, 5]. In a conventional FEL, coherent electromagnetic radiation is generated by subjecting an e-beam in vacuum to a transverse periodic wiggler magnetic field. The effect of the wiggler field is to provide coupling between the e-beam and electromagnetic radiation fields, which results in a ponderomotive force along the axis of the beam. This force leads to bunching of the electrons [6]. The subsequent interaction of the bunched beam with the incident electromagnetic wave gives rise to energy growth of the wave at the expense of the beam kinetic energy. The main merit of a FEL may be its high power capability and its tunability to a prescribed frequency. In addition, it may cover the whole spectrum of electromagnetic waves by adjusting the injected beam energy and the wiggler period. The frequency of radiation in a FEL is $\omega = k_w v_b/(1 - nv_b/c)$,

where k_w ($=2\pi/\lambda_w$) is the wiggler wavenumber, v_b is the electron beam velocity, and n is the refractive index of the cavity medium. Due to technical limitations of the wiggler wavelength ($\lambda \geq 1$ cm) and magnetic field strength (e.g., in a helical wiggler, <50 kG), a conventional FEL needs a very high-γ electron beam to generate a short wavelength and operates there with a low efficiency [7, 8]. This leads to beam requirements, such as higher energy, higher current and higher quality, as well as magnet requirements, such as a stronger and more precise magnetic field, very accurate wiggler wavelengths and alignment.

In recent years, much effort has been expended in the investigation of ion-channel pumped FELs [9–13]. The technique of ion-channel guiding has emerged as an effective method for focusing the electron beam; a relativistic e-beam injected into an underdense plasma (the plasma density is less than the beam density) can expel the plasma electrons outward to create an ion-channel, which has ideal focusing properties for e-beams. It is a cost effective alternative to the axial guide magnetic field in FELs, due to lower capital and operating expenses [14, 15]. Furthermore, it permits a beam current higher than the vacuum limit and helps in radiation guiding [16, 17]. One of the significant physical limitations of the ion-channel focusing regime is the ion-hose instability, in which transverse oscillations of the electron beam and ion-channel couple and grow [18]. This instability imposes a constraint on the useful pulse or propagation length. Furthermore, in the ion-channel regime the plasma density has to be smaller than the electron beam density in order to produce the ion-channel. This leads to serious limits on the gain of a FEL. It seems that these limitations may be suppressed when we use a plasma wave as a wiggler in FELs; the presence of the plasma opens up the possibility of employing the plasma eigenmodes as a wiggler for the excitation of shorter wavelengths. The plasma can significantly slow down the radiation mode, thereby relaxing the beam energy requirement considerably [19, 20]. As the plasma wave wiggler has a very short period, it allows the production of short waves using a beam with moderate electron energy. The presence of the plasma in the interaction region helps in the generation of higher powers in several ways. First, it allows beam currents in excess of the vacuum current limit via charge neutralization [21, 22]. Second, the electron bunching process can be enhanced by tuning the wave frequency close to the plasma frequency [23]. Third, a density-depleted plasma channel provides strong radiation guiding [24, 25]. Joshi *et al* [26] have studied the possibility of employing a Langmuir wave wiggler. Sharma and Tripathi [27] have investigated the whistler wave as a wiggler in the inner region of a FEL. Moreover, in a different work, these authors have studied the generation of high-frequency coherent radiation by a large amplitude upper hybrid wave [28]. Wen-Bing *et al* [29] have observed an enhancement in the gain and frequency of a plasma loaded FEL in the presence of high-density plasmas. The linear theory of a plasma-loaded helix-type traveling wave tube amplifier was studied by Kobayashi *et al* [30]. In this research, the role of the plasma on the gain and degree of concentration of the high-frequency field on the region of the plasma is considered, and strong gain enhancements are observed for frequencies in which hybrid plasma slow waves are formed. Recently, the generation of harmonics of laser radiation in plasmas has been studied by Ganeev [31], indicating new opportunities for the efficient generation of strong coherent short wavelength radiation.

In this paper, a magnetized plasma eigenmode has been employed as a wiggler. This wiggler propagates parallel to the relativistic e-beam. In our physical model, we assume that the plasma is collisionless. The beam pulse length is assumed to be short compared to the time for ions to neutralize the beam. The two-stream instability due to the relative motion of the beam and plasma electrons can be avoided if we consider the dimensions of the particle bunches to be small in comparison with the length of the plasma wave [24, 32]. Here, to confine the beam against the effects of self-fields, an axial guide magnetic field, $B_0\hat{\mathbf{z}}$, is employed. Another effect of the axial guide field is to increase the magnitude of the transverse wiggler-induced velocity resonantly when the Larmor period associated with the axial field is comparable to the plasma eigenmode period [33].

By passing a relativistic e-beam through a magnetized plasma channel, high-frequency electromagnetic radiation is generated by coupling the electromagnetic wave to the negative energy electrostatic beam modes. The negative energy electrostatic beam mode and the positive energy electromagnetic wave can strongly couple together, leading to an instability [34, 35]. During the course of the instability, the amplitudes of beam modes increases and the waves begin to trap electrons. Because of the relativistic effects on the mass of the electrons, the bounce period of the electrons trapped in the electrostatic potential well is long. During the bounce period, the unstable electromagnetic waves continue to grow to overshoot. This overshoot of the wave amplitudes results in further energy deposition into electromagnetic radiation [36]. A schematic diagram of an electron beam propagating through the magnetized plasma wave wiggler is shown in figure 1. Table 1 shows the plasma eigenmodes which can be used as a wiggler.

The organization of the paper is as follows. In section 2, electron trajectories in a magnetized plasma wave wiggler are presented. The effects of beam quality, such as axial energy spread and beam emittance on electron trajectories, are given in section 3. The self-electric and self-magnetic fields of the e-beam are also derived from Poisson's equation and Ampere's law, respectively. A self-consistent method for calculation of the self-magnetic field generated by the wiggler-induced transverse velocity is also presented. In section 4, the small-signal gain of the plasma wiggler FEL is derived, which has been generalized to the gain equation in the presence of beam self-fields. Finally, numerical studies and conclusions are described in section 5.

2. Electron trajectories

A relativistic e-beam propagating through a magnetized plasma channel can support several types of beam idler [37].

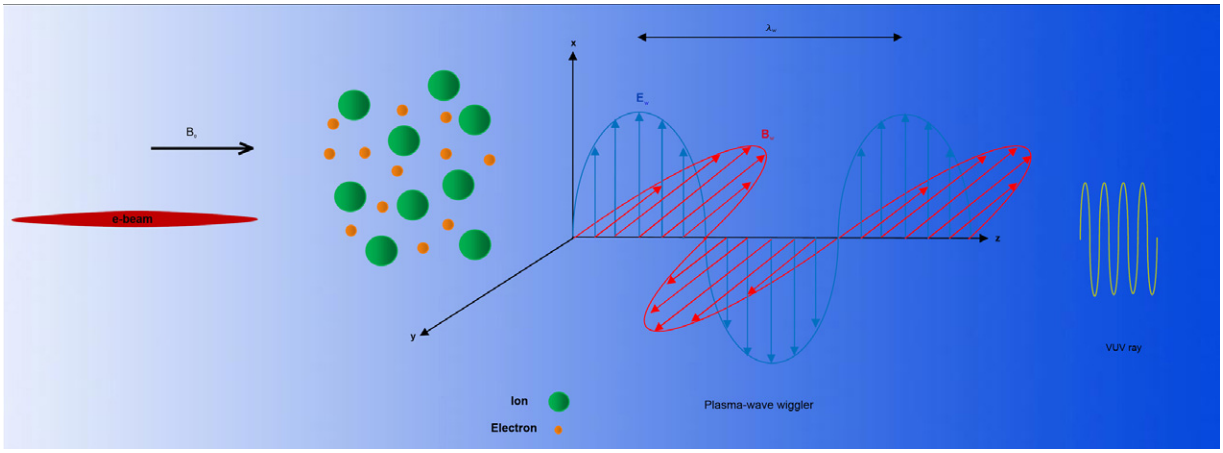

Figure 1. A schematic diagram of the propagation of an electron beam in the presence of the magnetized plasma wave wiggler.

Table 1. Plasma eigenmodes used as a wiggler in a FEL.

Plasma wave	(ω_s, k_s)
Right circularly polarized mode (Whistler mode) [27]	$\omega_s = ck_s \Big/ \sqrt{1 - \frac{\omega_p^2}{\omega_s(\omega_s - \omega_c)}}$
Left circularly polarized mode [63]	$\omega_s = ck_s \Big/ \sqrt{1 - \frac{\omega_p^2}{\omega_s(\omega_s + \omega_c)}}$
Alfven mode [63]	$\omega_s = v_A k_s$ (v_A, Alfven speed)
Langmuir mode [26]	$\omega_s^2 = \omega_p^2 + \frac{3}{2}k_s^2 v_{th}^2$ (v_{th}, thermal velocity of the plasma electrons)
Ion acoustic mode [32]	$\omega_s = v_s k_s$ (v_s, ion acoustic speed)
Upper hybrid mode [28]	$\omega_s^2 = \frac{1}{2}\left(\omega_p^2 + \omega_c^2 + \sqrt{\omega_p^2 + \omega_c^2 - \frac{4\omega_p^2\omega_c^2 k_{sz}^2}{k_{sz}^2 + k_{s\perp}^2}}\right)$

The most significant types are the negative energy space charge and cyclotron waves, as well as their harmonics. These waves couple energy from the e-beam into scattered radiation. Then [38],

$$\omega_r - \omega_s = (k_{mod} \pm k_r)v_b - \omega_i, \tag{1}$$

where ω_r, ω_s and ω_i are the radiation, pump and idler wave frequencies, k_r is the radiation wavenumber, v_b is the beam velocity, and $\pm$ signs correspond to forward/backward propagating waves. Moreover,

$$k_{mod} = \frac{\omega_s}{v_{ph}}\left(1 + \frac{v_b}{v_{ph}}\right), \tag{2}$$

is the modifying wavenumber of the pump wave, and v_{ph} is the phase velocity of the pump wave.

The configuration of interest consists of monoenergetic relativistic electron beam propagation through a magnetized plasma channel, which is given by

$$\mathbf{B}_s = \tfrac{1}{2}B_s \exp[i(k_s z - \omega_s t)](\hat{\mathbf{x}} + i\hat{\mathbf{y}}) + \mathrm{CC}, \tag{3}$$

$$\mathbf{E}_s = \frac{i}{2}\frac{\omega_s}{ck_s}B_s \exp[i(k_s z - \omega_s t)](\hat{\mathbf{x}} + i\hat{\mathbf{y}}) + \mathrm{CC}, \tag{4}$$

where B_s is the amplitude of the plasma magnetic field, ω_s and k_s denote the frequency and wavenumber of the plasma pump wave, z and t are the longitudinal position and time, respectively, and CC indicates the complex conjugate.

The dynamics of an electron with rest mass m and charge $-e$ moving with velocity $\mathbf{V}$ in the presence of a magnetized plasma wave can be expressed as [39]

$$\frac{d\mathbf{V}}{dt} = -\frac{e}{m\gamma}\left[\left(\mathbf{I} - \frac{1}{c^2}\mathbf{VV}\right)\cdot\mathbf{E}_s + \frac{1}{c}\mathbf{V}\times(B_0\hat{\mathbf{z}} + \mathbf{B}_s)\right], \tag{5}$$

$$\frac{d\gamma}{dt} = -\frac{e}{mc^2}\mathbf{V}\cdot\mathbf{E}_s, \tag{6}$$

where $\mathbf{I}$ is a unit dyadic, γ is the relativistic factor and c is the speed of light in vacuum. For convenience, we introduce the wiggler frame as

$$\hat{\mathbf{e}}_1 = \hat{\mathbf{x}}\cos(k_s z - \omega_s t) - \hat{\mathbf{y}}\sin(k_s z - \omega_s t), \tag{7}$$

$$\hat{\mathbf{e}}_2 = \hat{\mathbf{x}}\sin(k_s z - \omega_s t) + \hat{\mathbf{y}}\cos(k_s z - \omega_s t), \tag{8}$$

$$\hat{\mathbf{e}}_3 = \hat{\mathbf{z}}. \tag{9}$$

Now, we can write the scalar equations in the wiggler frame as

$$\frac{d\beta_1}{d\tau} = -\omega_c\beta_2 - \Omega_s\beta_1\beta_2\beta_s + \beta_2\beta_3 - \beta_2\beta_s, \tag{10}$$

$$\frac{d\beta_2}{d\tau} = \Omega_s\beta_s - \Omega_s\beta_3 + \omega_c\beta_1 - \Omega_s\beta_2^2\beta_s - \beta_1\beta_3 + \beta_1\beta_s, \tag{11}$$

$$\frac{d\beta_3}{d\tau} = \Omega_s\beta_2 - \beta_3\beta_2\beta_s\Omega_s, \tag{12}$$

$$\frac{d\gamma}{d\tau} = \gamma\Omega_s\beta_2\beta_s, \tag{13}$$

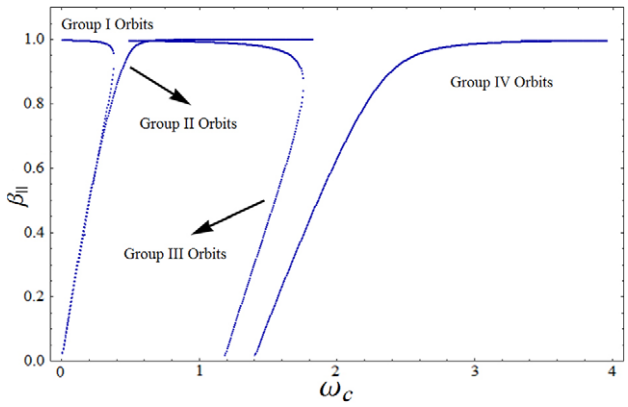

Figure 2. Graph of the normalized axial velocity, $\beta_\parallel$, as a function of the normalized cyclotron frequency, ω_c, for orbits of groups I–IV. The chosen parameters are $\omega_b = 0.08$, $\omega_p = 0.8$, $\gamma = 200$ and $\Omega_s = 0.07$.

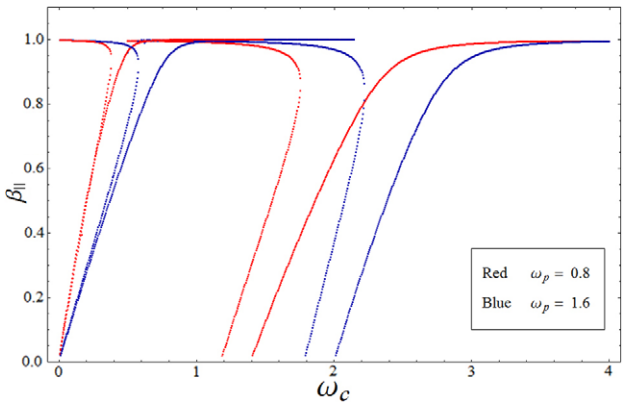

Figure 3. Graph of the normalized axial velocity, $\beta_\parallel$, as a function of ω_c, for $\omega_p = 0.8$ and $\omega_p = 1.6$. The chosen parameters are $\omega_b = 0.08$, $\gamma = 200$ and $\Omega_s = 0.07$.

where $\beta_i = v_i/c$ is the normalized beam velocity, $\beta_s(=\omega_s/ck_s)$ is the normalized phase velocity of the plasma pump wave, $\omega_c = (eB_0/\gamma mc^2 k_s)$ is the normalized cyclotron frequency of the e-beam, and $\Omega_s = (eB_s/\gamma mc^2 k_s)$.

The steady-state electron orbits for this configuration are found under the requirement that the total energy of the electron remains constant ($d\gamma/d\tau = 0$) [33, 39]. This implies that the normalized transverse velocity in the wiggler frame can be written as

$$\beta_w = \frac{\Omega_s(\beta_\parallel - \beta_s)}{\omega_c - (\beta_\parallel - \beta_s)}, \tag{14}$$

where $\beta_\parallel(=\beta_3)$ is the normalized axial velocity of the e-beam. The injection of the beam on the steady-state trajectories ensures that the wave–particle resonance will be maintained over an extended interaction length, and maximizes the gain of interaction [33]. Since the energy is a constant for the steady-state trajectories, β_w and $\beta_\parallel$ are related through $\beta_w^2 + \beta_\parallel^2 = 1 - \gamma^{-2}$. For a monoenergetic e-beam, the phase velocity of the plasma wave is determined in a self-consistent fashion [33, 39] by the dielectric properties of the medium as

$$\beta_s^2 - 1 - \frac{\omega_b^2(\beta_\parallel - \beta_s)}{\omega_c - (\beta_\parallel - \beta_s)} + \frac{\gamma\omega_p^2\beta_s}{\gamma\omega_c + \beta_s} = 0, \tag{15}$$

where $\omega_b = (4\pi e^2 n_b/\gamma mc^2 k_s^2)^{1/2}$ is the normalized beam frequency, $\omega_p = (4\pi e^2 n_p/\gamma mc^2 k_s^2)^{1/2}$ is the normalized plasma electron frequency, and n_b and n_p are the beam and plasma density, respectively. In order to operate in the cold (monoenergetic) beam regime, the axial velocity spread of the beam most be small. The effects of the normalized cyclotron and plasma frequencies on the normalized axial velocity of the e-beam are shown in figures 2 and 3.

3. Beam quality

The quality of e-beam is critical to the operation of a FEL. The FEL interaction is driven by axial bunching of electrons and requires the matching of their axial velocity to the phase velocity of the ponderomotive wave [40]. In a real situation, the energy spread, emittance and self-fields of the electron beam are the source of a spread in the axial velocity of the beam that can generally affect the gain and efficiency of FELs. The relationship between the beam emittance and the beam energy spread can be expressed as [41]

$$\frac{\Delta\gamma_z}{\gamma_0} = \frac{1}{2}\left(\frac{\gamma_z}{\gamma_0}\right)^3\left(\frac{\gamma_0\beta_0\epsilon}{r_b}\right)^2, \tag{16}$$

where $\gamma_0 = (1 - \beta_0^2)^{-1/2}$, β_0 is the total normalized velocity, $\gamma_z = (1 - \beta_\parallel^2)^{-1/2}$, r_b is the beam radius and $\epsilon_n(=\gamma_0\beta_0\epsilon)$ is the normalized emittance of electron beam. Furthermore, the axial momentum spread can be related to the axial energy spread using the relation [41, 42],

$$\frac{\Delta\gamma_z}{\gamma_0} = 1 - \left(1 + 2\gamma_0^2\beta_0^2\frac{\Delta P_z}{P_0}\right)^{-1/2}, \tag{17}$$

where $P_0 = \gamma_0 mc\beta_0$ is the total momentum and ΔP_z is the axial momentum spread of the beam. Considering $P_0^2 = P_{z0}^2 + P_{w0}^2$, $\Delta P_z = P_z - P_{0z}$, and $\beta_z \approx 1 - \frac{1}{2\gamma_0^2} - \frac{\beta_w^2}{2}$ (for $\gamma_0 \gg 1$), we can rewrite the above equation as

$$\frac{\Delta\gamma_z}{\gamma_0} = 1 - \left[1 + \frac{2(\gamma_0^2 - 1)}{\sqrt{1 - \gamma_0^{-2}}}\left(1 - \frac{1}{2\gamma_0^2} - \frac{\beta_w^2}{2} - \beta_\parallel\right)\right]^{-1/2}, \tag{18}$$

where β_w is defined in equation (14).

The self-fields generated by the charge and current densities of the electron beam are known to have a significant effect on the operation of the FEL. The self-fields can either enhance or reduce the external pump field, depending on the latter's phase velocity and the strength of the longitudinal guide magnetic field [43–45]. The first-order self-magnetic field generated by the wiggler-induced transverse velocity was calculated by Freund *et al* [46]. Hafizi and Roberson found that self-fields tend to reduce the spread in the axial velocity of the beam electrons, i.e., self-fields effectively cool the beam [47]. In addition, they have shown that the contributions due to emittance (or energy spread) and self-fields have opposite signs. This leads to an improvement in beam quality due to beam self-fields [47, 48].

We make the assumption of a uniform electron beam density profile $n_b(r) = n_b = \text{const.}$ for $r \le r_b$ and $n_b(r) = 0$ for $r > r_b$, where n_b is the number density of the electrons and r_b is the radius of the beam. The self-electric field induced by the charge density of the non-neutral electron beam can be obtained by solving Poisson's equation,

$$\nabla \cdot \mathbf{E}_{sf} = -4\pi e n_b(r). \tag{19}$$

Solving the above equation, we obtain

$$\mathbf{E}_{sf} = -2\pi e n_b (x\hat{\mathbf{e}}_\mathbf{x} + y\hat{\mathbf{e}}_\mathbf{y}). \tag{20}$$

The lowest-order representation for the self-magnetic field is obtained under the assumption that the beam propagates paraxially with $\mathbf{V} = v_\parallel \hat{\mathbf{z}}$ for $r \le r_b$ and is zero otherwise. In this case, the self-magnetic field is determined by Ampere's law,

$$\nabla \times \mathbf{B}_{sf} = \frac{4\pi}{c}\mathbf{J}, \tag{21}$$

where $\mathbf{J} = -en_b c\beta_\parallel \hat{\mathbf{z}}$ is the electron beam current density, and $\beta_\parallel = v_\parallel/c$ is the normalized axial electron velocity. The solution of above equation can be expressed as

$$\mathbf{B}_{sf} = 2\pi e n_b \beta_\parallel (y\hat{\mathbf{x}} - x\hat{\mathbf{y}}). \tag{22}$$

An analysis of the relativistic motion of an electron beam in the FEL with a plasma wave wiggler and an axial guide magnetic field with regards to the self-electric and self-magnetic fields of the beam will be based on equations (5) and (6). Thus, the scalar equations of motion are given by

$$\frac{d\beta_1}{d\tau} = -\omega_c\beta_2 - \Omega_s\beta_1\beta_2\beta_s + \beta_2\beta_3 - \beta_2\beta_s - \beta_3^2\omega_b^2\chi_1 + \omega_b^2\chi_1 - \beta_1\beta_2\omega_b^2\chi_2 - \beta_1^2\omega_b^2\chi_1, \tag{23}$$

$$\frac{d\beta_2}{d\tau} = \Omega_s\beta_s - \Omega_s\beta_3 + \omega_c\beta_1 - \Omega_s\beta_2^2\beta_s - \beta_1\beta_3 + \beta_1\beta_s - \beta_3^2\omega_b^2\chi_2 + \omega_b^2\chi_2 - \beta_1\beta_2\omega_b^2\chi_1 - \beta_2^2\omega_b^2\chi_2, \tag{24}$$

$$\frac{d\beta_3}{d\tau} = \Omega_s\beta_2 - \beta_3\beta_2\beta_s\Omega_s, \tag{25}$$

and

$$\frac{d\gamma}{d\tau} = \gamma\Omega_s\beta_2\beta_s + \gamma\omega_b^2\chi_1\beta_1 + \gamma\omega_b^2\chi_2\beta_2, \tag{26}$$

where $\chi_i = k_s x_i$ denotes the component of the position of the electron in the wiggler frame. The steady-state orbits for this configuration are obtained as $\vec{\beta} = \beta_{0w}\hat{\mathbf{e}}_\mathbf{1} + \beta_\parallel \hat{\mathbf{e}}_\mathbf{3}$, where

$$\beta_{0w} = \frac{\Omega_s(\beta_\parallel - \beta_s)^2}{\omega_b^2(1-\beta_\parallel^2) + \omega_c(\beta_\parallel - \beta_s) - (\beta_\parallel - \beta_s)^2}. \tag{27}$$

The self-magnetic field that is induced by the transverse velocity is known as the wiggler-induced self-magnetic field ($\mathbf{B}_{sw}$). Assume that the wiggler-induced self-magnetic field is proportional to the wiggler magnetic field (i.e., $\mathbf{B}_{sw}^{(1)} = \lambda^{(1)}\mathbf{B}_s$). As a result, the coefficient $\lambda^{(1)}$ can be derived from Ampere's law,

$$\lambda^{(1)} = \frac{-2\omega_b^2(\beta_\parallel - \beta_s)^2}{\omega_b^2(1-\beta_\parallel^2) + \omega_c(\beta_\parallel - \beta_s) - (\beta_\parallel - \beta_s)^2}. \tag{28}$$

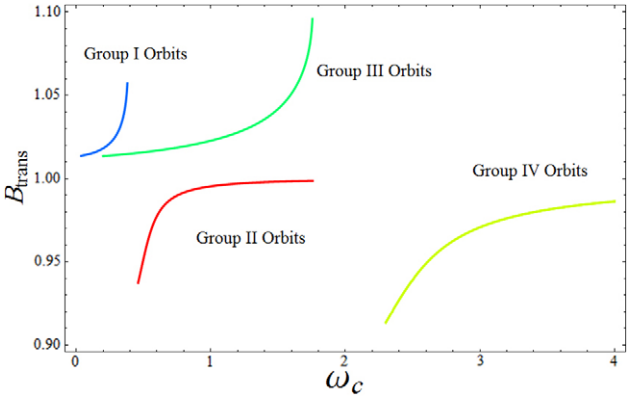

Figure 4. Graph of the total transverse magnetic fields, $\mathbf{B}_{trans.}$, as a function of the normalized cyclotron frequency, ω_c, for orbits of groups I–IV. The chosen parameters are $\omega_b = 0.08$, $\omega_p = 0.8$, $\gamma = 200$ and $\Omega_s = 0.07$.

The field $\mathbf{B}_{sw}^{(1)}$ also generates a transverse velocity named the wiggler-induced transverse velocity and its magnitude can be written as $\beta_{sw}^{(1)} = (1 + \lambda^{(1)})\beta_{0w}$. Consequently, this velocity produces a new self-magnetic field $\mathbf{B}_{sw}^{(2)} = \lambda^{(2)}\mathbf{B}_s$ and so on. Using Ampere's law, we can find [49, 50]

$$\lambda^{(n)} = \lambda^{(1)}[1 + \lambda^{(1)} + (\lambda^{(1)})^2 + (\lambda^{(1)})^3 + \cdots + (\lambda^{(1)})^{n-1}]. \tag{29}$$

This is a geometric series and for $n \to \infty$ the series is convergent if $|\lambda^{(1)}| < 1$, which is a restriction for validity of this method in high electron beam density. Therefore, the total wiggler-induced self-magnetic field $\mathbf{B}_{sw}$ can be found as $\mathbf{B}_{sw} = \lim_{n\to\infty}\lambda^{(n)}\mathbf{B}_s = \lambda^{(1)}\mathbf{B}_s/(1-\lambda^{(1)})$. As a result,

$$\begin{aligned}\mathbf{B}_{sw} &= \sigma\mathbf{B}_s \\ &= [-2\omega_b^2(\beta_\parallel - \beta_p)^2][\omega_b^2(1-\beta_\parallel^2) + \Omega_0(\beta_\parallel - \beta_p) \\ &\quad - (1-2\omega_b^2)(\beta_\parallel - \beta_p)^2]^{-1}\mathbf{B}_s.\end{aligned} \tag{30}$$

The magnitude of the normalized wiggler-induced transverse electron velocity can also be obtained from $\beta_{sw} = \lim_{n\to\infty}[1 + \lambda^{(n)}]\beta_{0w}$. Thus, we have

$$\beta_{sw} = \frac{\Omega_s(\beta_\parallel - \beta_s)^2}{\omega_b^2(1-\beta_\parallel^2) + \omega_c(\beta_\parallel - \beta_s) - (1-2\omega_b^2)(\beta_\parallel - \beta_s)^2}. \tag{31}$$

The effect of the normalized cyclotron frequency, ω_c, on the normalized total transverse magnetic field, $(\mathbf{B}_{sw} + \mathbf{B}_s)/\mathbf{B}_s$, is shown in figure 4.

It should be mentioned that by conditioning an electron beam through establishing a correlation between transverse action and energy within the beam, the performance of FELs can be dramatically improved [51]. Conditioning enhances the FEL gain by reducing the axial velocity spread within the electron bunch generated over the wiggler, due to both energy spread and finite transverse emittance [52, 53]. Recently, a plasma channel beam conditioner for FELs has been proposed by Penn *et al* [54], in which strong transverse focusing produced by the plasma channel allows the optimal correlation to be achieved. Furthermore, a number

of techniques have been proposed to pre-bunch the electron beam for increasing the efficiency in microwave tubes [55]. The concept relies on the fact that, if the beam is bunched on scale lengths comparable to or shorter than the desired wavelength, then the resonant wavelength is strongly excited without a drive signal [56]. The results obtained by Freund *et al* [57] indicate that partial pre-bunching of an electron beam in FELs results in substantial increases in the efficiency, shortening the saturation length and giving an improvement in longitudinal coherence.

4. Small-signal gain

Now consider electromagnetic radiation co-propagating with the electron in the interaction region. The electric and magnetic fields of the radiation can be written as [58, 59]

$$\mathbf{E}_\mathrm{r} = E_\mathrm{r}\cos\zeta\,\hat{\mathbf{x}} - E_\mathrm{r}\sin\zeta\,\hat{\mathbf{y}}, \tag{32}$$

$$\mathbf{B}_\mathrm{r} = E_\mathrm{r}\sin\zeta\,\hat{\mathbf{x}} + E_\mathrm{r}\cos\zeta\,\hat{\mathbf{y}}, \tag{33}$$

where $\zeta = k_\mathrm{r}z - \omega_\mathrm{r}t + \phi$, k_r is the wavenumber, ω_r is the angular frequency of the radiation wave, E_r is the amplitude of the wave and ϕ is the phase constant. The phase ϕ determines the initial position of the electron relative to the optical (radiation) wave. In the wiggler frame, these equations can be expressed as

$$\mathbf{E}_\mathrm{r} = E_\mathrm{r}\cos\psi\hat{\mathbf{e}}_1 - E_\mathrm{r}\sin\psi\hat{\mathbf{e}}_2, \tag{34}$$

$$\mathbf{B}_\mathrm{r} = E_\mathrm{r}\sin\psi\hat{\mathbf{e}}_1 + E_\mathrm{r}\cos\psi\hat{\mathbf{e}}_2, \tag{35}$$

where $\psi = (k_\mathrm{r} - k_\mathrm{s})z - (\omega_\mathrm{r} - \omega_\mathrm{s})t + \phi$. The electron equation of the motion for the normalized velocity components in the presence of the radiation fields may be written in the scalar form,

$$\frac{\mathrm{d}\beta_1}{\mathrm{d}\tau} = -\omega_\mathrm{c}\beta_2 - \Omega_\mathrm{s}\beta_1\beta_2\beta_\mathrm{s} + \beta_2\beta_3 - \beta_2\beta_\mathrm{s} + (\beta_3 - 1)\widetilde{E}_\mathrm{r}\cos\psi, \tag{36}$$

$$\frac{\mathrm{d}\beta_2}{\mathrm{d}\tau} = \Omega_\mathrm{s}\beta_\mathrm{s} - \Omega_\mathrm{s}\beta_3 + \omega_\mathrm{c}\beta_1 - \Omega_\mathrm{s}\beta_2^2\beta_\mathrm{s} - \beta_1\beta_3 + \beta_1\beta_\mathrm{s} + (1 - \beta_3)\widetilde{E}_\mathrm{r}\sin\psi, \tag{37}$$

$$\frac{\mathrm{d}\beta_3}{\mathrm{d}\tau} = \Omega_\mathrm{s}\beta_2 - \beta_3\beta_2\beta_\mathrm{s}\Omega_\mathrm{s} + \widetilde{E}_\mathrm{r}(\sin\psi\beta_2 - \cos\psi\beta_1), \tag{38}$$

where $\widetilde{E}_\mathrm{r} = eE_\mathrm{r}/\gamma mc^2k_\mathrm{s}$ is the normalized amplitude of the radiation wave.

For the solution of equations (36)–(38), we consider that for β_3 close to one, the last term in equations (36) and (37) due to the transverse optical force acting on electrons may be neglected in comparison with the other terms, which are due to the transverse forces of the wiggler fields. Therefore, to a very good approximation, the transverse electron velocity components in the presence of the radiation fields may be taken as the steady-state solutions. Using equation (14) along with the energy conservation relation $\beta_\mathrm{w}^2 + \beta_\parallel^2 = 1 - \gamma^{-2}$, for $\gamma \gg 1$, we obtain

$$\beta_3 \simeq 1 - \frac{1}{2\gamma^2} - \frac{\Omega_\mathrm{s}^2(\beta_\parallel - \beta_\mathrm{s})^2}{2(\omega_\mathrm{c} - (\beta_\parallel - \beta_\mathrm{s}))^2}. \tag{39}$$

The energy exchange of the electron with the radiation field is given by

$$\langle\dot{\gamma}\rangle = \frac{\mathrm{d}\gamma}{\mathrm{d}t} = -\frac{e}{mc^2k_\mathrm{s}}\beta\cdot\mathbf{E} = -\gamma\beta_\mathrm{w}\widetilde{E}_\mathrm{r}\cos\psi. \tag{40}$$

Averaging this equation over all phases yields $\langle\dot{\gamma}\rangle_\phi = 0$; therefore, to the first order, there is no net transfer of energy between the electron beam and the optical wave. The second-order correction will consist of accounting for the fact that as an individual electron (with phase ϕ) gains or loses energy, its position relative to the unperturbed position ($z = c\beta_\parallel t$) is advanced or retarded. Thus, the unperturbed position $z = c\beta_\parallel t$ must be replaced by

$$z(t) = c\beta_\parallel t + c\int_0^t \Delta\beta_3(t')\,\mathrm{d}t', \tag{41}$$

where $\Delta\beta_3(t) = \int_0^t \dot{\beta}_3(t')\,\mathrm{d}t'$ is the change of β_3 relative to the unperturbed state. The substitution of $\dot{\beta}_3$ in the normalized form of $z(t)$ will yield

$$\Lambda_z(\tau) = \beta_\parallel\tau - \frac{\widetilde{E}_\mathrm{r}\beta_\mathrm{w}}{\gamma^2\Omega^2}\left[1 - \frac{\gamma^2\Omega_\mathrm{s}^2(\beta_\parallel - \beta_\mathrm{s})^3}{(\omega_\mathrm{c} - (\beta_\parallel - \beta_\mathrm{s}))^3}\right] \times [\cos(\Omega\tau + \phi) - \cos\phi + \Omega\tau\sin\phi], \tag{42}$$

where $\tau = ck_\mathrm{s}t$, $\Omega = (\widetilde{k}_\mathrm{r} - 1)\beta_\parallel + (1 - \widetilde{\omega}_\mathrm{r})\beta_\mathrm{s}$, and $\widetilde{k}_\mathrm{r} = k_\mathrm{r}/k_\mathrm{s}$ and $\widetilde{\omega}_\mathrm{r} = \omega_\mathrm{s}/ck_\mathrm{s}$ are the normalized wavenumber and frequency of the radiation wave.

The substitution of $\Lambda_z(\tau)$ in the ψ of equation (40) leads to

$$\langle\dot{\gamma}\rangle = \gamma\widetilde{E}_\mathrm{r}\beta_\mathrm{w}\cos[(\Omega\tau + \phi) - \Delta\phi], \tag{43}$$

where the phase slippage $\Delta\phi$ is expressed by

$$\Delta\phi = \frac{\widetilde{E}_\mathrm{r}\beta_\mathrm{w}(1 - \widetilde{k}_\mathrm{r})}{\gamma^2\Omega^2}\left[1 - \frac{\gamma^2\Omega_\mathrm{s}^2(\beta_\parallel - \beta_\mathrm{s})^3}{(\omega_\mathrm{c} - (\beta_\parallel - \beta_\mathrm{s}))^3}\right] \times [\cos(\Omega\tau + \phi) - \cos\phi + \Omega\tau\sin\phi]. \tag{44}$$

Taking the average of energy exchange from above equation over all phases ϕ, we obtain

$$\langle\dot{\gamma}\rangle_\phi = \frac{\widetilde{E}_\mathrm{r}^2\beta_\mathrm{w}^2(1 - \widetilde{k}_\mathrm{r})}{2\gamma\Omega^2}\left[1 - \frac{\gamma^2\Omega_\mathrm{s}^2(\beta_\parallel - \beta_\mathrm{s})^3}{(\omega_\mathrm{c} - (\beta_\parallel - \beta_\mathrm{s}))^3}\right] \times (\Omega\tau\cos\Omega\tau - \sin\Omega\tau). \tag{45}$$

Integrating the above equation over the electron transit time through the wiggler interaction length, the average change in γ per electron becomes

$$\langle\Delta\gamma\rangle_\phi = \int_0^{T=k_\mathrm{s}L/\beta_\parallel}\langle\dot{\gamma}\rangle_\phi\,\mathrm{d}\tau, \tag{46}$$

where L is the FEL interaction length and T is the normalized electron transit time through the wiggler interaction length. The change in electromagnetic power in one transit is $\triangle P_\mathrm{r} = -\frac{I}{e}mc^2\langle\Delta\gamma\rangle_\phi$, where I is the average electron beam current. The small-signal gain is defined by $G = \triangle P_\mathrm{r}/P_\mathrm{r}$, where $P_\mathrm{r} = (c\pi r_\mathrm{b}^2E_\mathrm{r}^2)/4\pi$ is the electromagnetic power [33, 45, 54]. Thus,

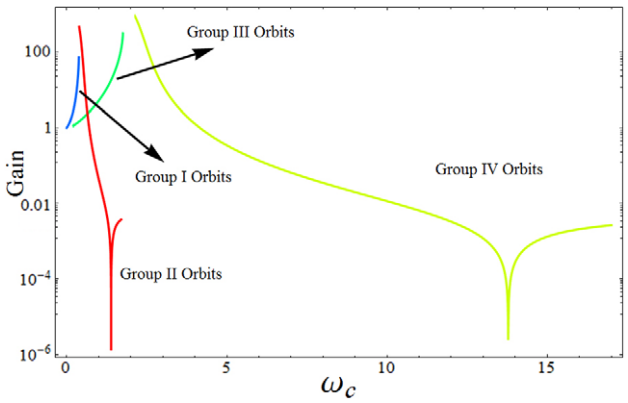

Figure 5. Graph of the normalized gain, $|G/G_0|$, as a function of the normalized cyclotron frequency, ω_c. The chosen parameters are $\omega_b = 0.08$, $\omega_p = 0.8$, $\gamma = 200$ and $\Omega_s = 0.07$.

the small-signal gain of the magnetized plasma wiggler can be expressed as

$$G = \frac{2mc^2\pi n_b \widetilde{E}_r^2(\widetilde{k}_r - 1)L^3k_s^3\gamma}{(\gamma E_r\beta_\parallel)^2}\left[\frac{\Omega_s(\beta_\parallel - \beta_s)}{\omega_c - (\beta_\parallel - \beta_s)}\right]^2 \times \left[1 - \frac{\gamma^2\Omega_s^2(\beta_\parallel - \beta_s)^3}{(\omega_c - (\beta_\parallel - \beta_s))^3}\right] \times \frac{(2 - 2\cos\Omega T - \Omega T\sin\Omega T)}{\Omega^3 T^3}. \quad (47)$$

Using a similar method, we can derive the small-signal gain of the magnetized plasma wiggler in the presence of self-electric and self-magnetic fields of the electron beam; the normalized components of electron velocity in the presence of the self-fields can be written as

$$\frac{d\beta_1}{d\tau} = -\omega_c\beta_2 - \Omega_s(1+\sigma)\beta_1\beta_2\beta_s + \beta_2\beta_3 - \beta_2\beta_s + \omega_b^2\chi_1 - \beta_3^2\omega_b^2\chi_1 - \beta_1\beta_2\omega_b^2\chi_2 - \beta_1^2\omega_b^2\chi_1 - \widetilde{E}_r\cos\psi(1-\beta_3), \quad (48)$$

$$\frac{d\beta_2}{d\tau} = \Omega_s(1+\sigma)\beta_s - \Omega_s(1+\sigma)\beta_3 + \omega_c\beta_1 - \Omega_s(1+\sigma)\beta_2^2\beta_s - \beta_1\beta_3 + \beta_1\beta_s + \omega_b^2\chi_2 - \beta_3^2\omega_b^2\chi_2 - \beta_1\beta_2\omega_b^2\chi_1 - \beta_2^2\omega_b^2\chi_2 + \widetilde{E}_r\sin\psi(1-\beta_3), \quad (49)$$

$$\frac{d\beta_3}{d\tau} = \Omega_s(1+\sigma)\beta_2 - \beta_3\beta_2\beta_s\Omega_s(1+\sigma) - \beta_1\widetilde{E}_r\cos\psi + \beta_2\widetilde{E}_r\sin\psi. \quad (50)$$

The energy exchange of the electron with the radiation fields is obtained from

$$\frac{d\gamma}{d\tau} = -\gamma\widetilde{E}_r\beta_{sw}\cos\psi, \quad (51)$$

where β_{sw} is the normalized wiggler-induced transverse velocity, equation (31). Taking the average of energy

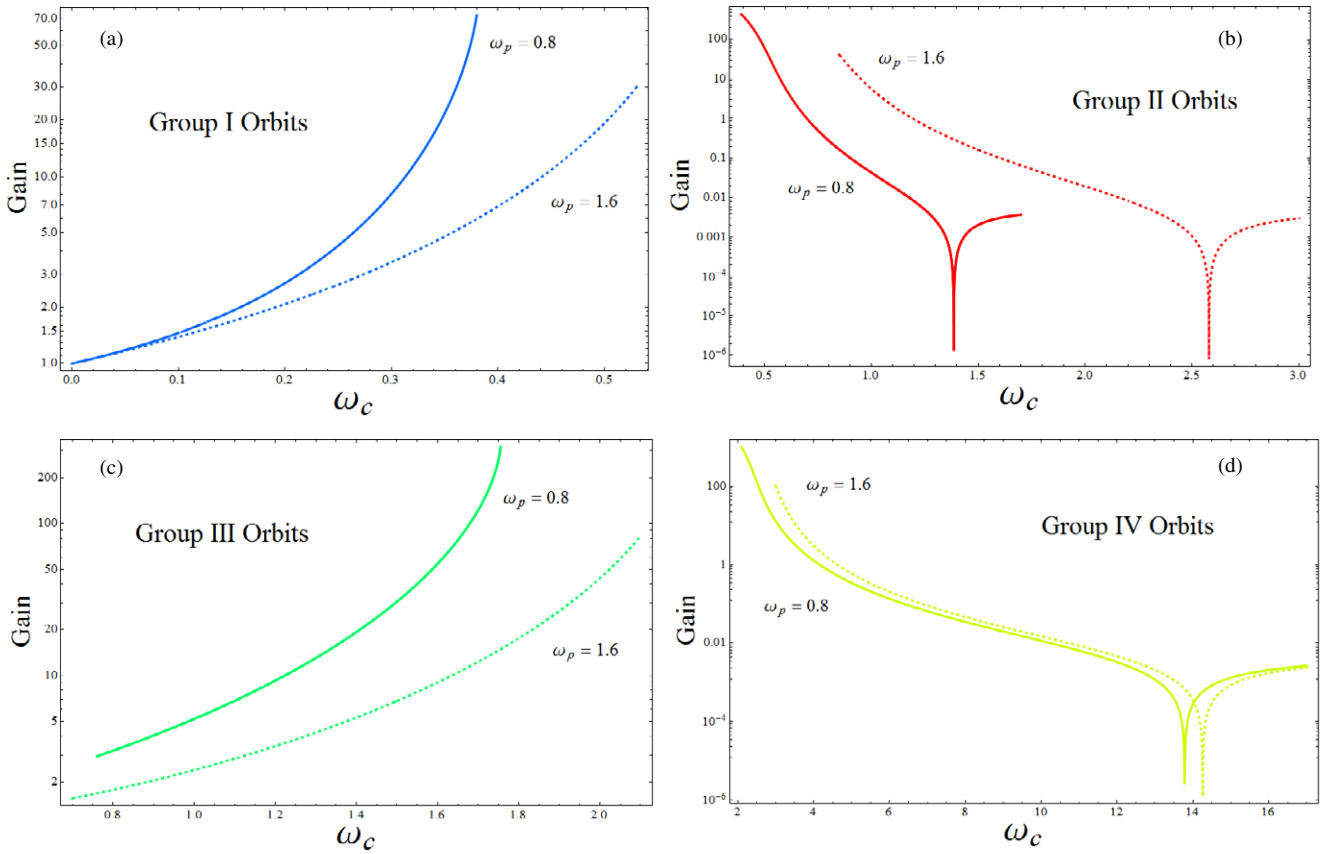

Figure 6. Graph of the gain ratio, $|G/G_0|$, as a function of the normalized cyclotron frequency, ω_c, for $\omega_p = 0.8$ and $\omega_p = 1.6$ in orbits of (a) group I, (b) group II, (c) group III and (d) group IV. The chosen parameters are $\omega_b = 0.08$, $\gamma = 200$ and $\Omega_s = 0.07$.

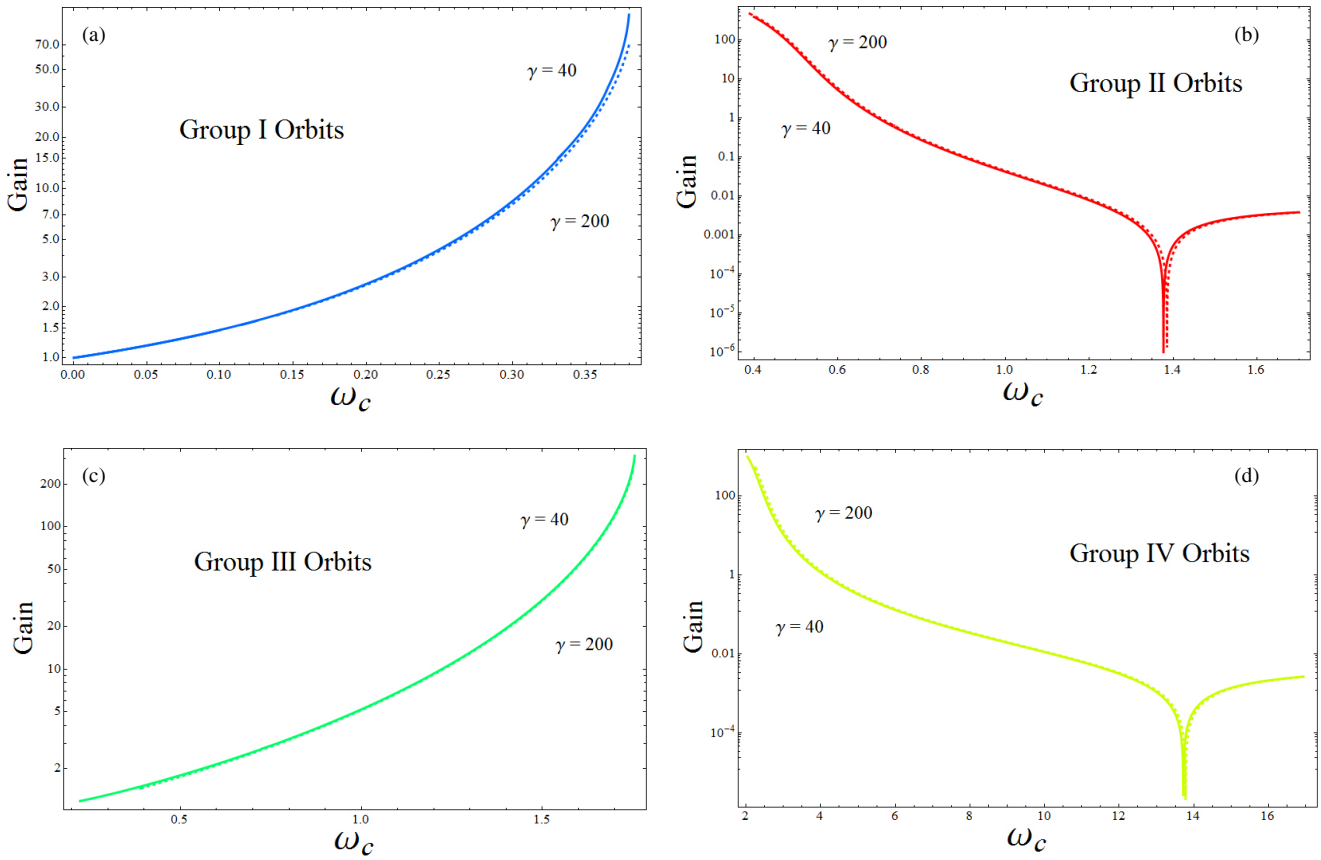

Figure 7. Graph of the normalized gain, $|G/G_0|$, as a function of the normalized cyclotron frequency, ω_c, for $\gamma = 40$ and $\gamma = 200$ in orbits of (a) group I, (b) group II, (c) group III and (d) group IV. The chosen parameters are $\omega_b = 0.08$, $\omega_p = 0.8$ and $\Omega_s = 0.07$.

exchange over all phases ϕ, we get

$$\langle\dot{\gamma}\rangle_\phi = \frac{\widetilde{E}_r^2\beta_{sw}^2(1-\widetilde{k}_r)}{2\gamma\Omega^2}[1-\{\gamma^2\Omega_s^2(\beta_\parallel-\beta_s)^6\}\{[\omega_b^2(1-\beta_\parallel^2) + \omega_c(\beta_\parallel-\beta_s) - (1-2\omega_b^2)(\beta_\parallel-\beta_s)^2]^3\}^{-1}] \times (\Omega\tau\cos\Omega\tau - \sin\Omega\tau). \quad (52)$$

The small-signal gain is obtained by

$$G = \frac{\Delta P_r}{P_r} = \frac{-mc^3 n_b \pi r_b^2 \beta_\parallel}{c\pi r_b^2 E_r^2/4\pi}\int_0^{T=k_sL/\beta_\parallel}\langle\dot{\gamma}\rangle_\phi\,\mathrm{d}\tau. \quad (53)$$

Thus, the small-signal gain of the magnetized plasma wiggler in the presence of self-fields of the e-beam can be expressed as

$$G_{self} = \frac{2mc^2\pi n_b\widetilde{E}_r^2(\widetilde{k}_r-1)L^3k_s^3\gamma}{(\gamma E_r\beta_\parallel)^2} \times [\{\Omega_s(\beta_\parallel-\beta_s)^2\}\{\omega_b^2(1-\beta_\parallel^2)+\omega_c(\beta_\parallel-\beta_s) - (1-2\omega_b^2)(\beta_\parallel-\beta_s)^2\}^{-1}]^2 \times [1-\{\gamma^2\Omega_s^2(\beta_\parallel-\beta_s)^6\}\{[\omega_b^2(1-\beta_\parallel^2) + \omega_c(\beta_\parallel-\beta_s) - (1-2\omega_b^2)(\beta_\parallel-\beta_s)^2]^3\}^{-1}] \times \frac{(2-2\cos\Omega T-\Omega T\sin\Omega T)}{\Omega^3T^3}. \quad (54)$$

5. Numerical studies and conclusion

A numerical study of electron trajectories and gain in the magnetized plasma wiggler has been made. In this section graphs of the normalized axial velocity of the e-beam, $\beta_\parallel$, versus the normalized cyclotron frequency, ω_c, are shown in figures 2 and 3 respectively. The chosen parameters for figure 2 are $\gamma = 200$, $\Omega_s = 0.07$, $\omega_b = 0.08$, and $\omega_p = 0.8$. If we assume $\gamma = 200$ (∼100 MeV) and $\lambda_s(=2\pi/k_s) = 4$ mm, then $\omega_b = 0.08$, $\omega_p = 1.2$ and $\omega_c = 0.2$ are equivalent to a beam density of $n_b = 0.89\times10^{12}$ cm^{-3}, a plasma density $n_p = 1.9\times10^{16}$ cm^{-3}, and an axial magnetic field strength $B_0 = 10.7$ kG, respectively. As seen in figure 2, group I orbits occur when $\omega_c < 0.87$, and appear to be multivalued functions of the cyclotron frequency. In contrast, the solutions for group II orbits are single valued in terms of the cyclotron frequency. In this group, $\beta_\parallel$ increases with increasing cyclotron frequency. The behavior of group III orbits is similar to the group I orbits, i.e., it is a multivalued function of the cyclotron frequency. The group IV orbits are also in accordance with the group II orbits; $\beta_\parallel$ increases with increasing ω_c. In figure 3, electron orbits have been depicted for the higher plasma density, i.e., $\omega_p = 1.6$. As shown, when the plasma density increases, the electron orbits shift to the right, i.e., to higher cyclotron frequencies. Similar results on electron orbits (group I and group II orbits) in conventional FELs (such as helical, planar and electromagnetically pumped FELs) have been obtained

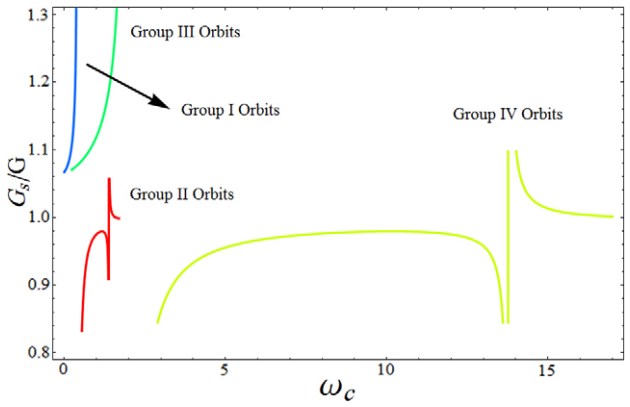

Figure 8. Graph of the normalized gain, $|G_{\rm self}/G|$, as a function of the normalized cyclotron frequency, $\omega_{\rm c}$. The chosen parameters are $\omega_{\rm b} = 0.08$, $\omega_{\rm p} = 0.8$, $\gamma = 200$ and $\Omega_{\rm s} = 0.07$.

by Freund *et al* [60–62], but what makes a difference between our finding and those of Freund is that the electron orbits in the magnetostatic and electromagnetic wigglers have fixed starting points (i.e., $\omega_{\rm c} = 0$ in the magnetostatic wigglers [60, 61] and $\omega_{\rm c} \approx 1$ in the electromagnetic wiggler [62]), and these orbits are not displaced upon varying the device parameters (for example, $\omega_{\rm b}$ and γ). But in the presence of the plasma wave wiggler, it has been observed that by varying the plasma density, electron orbits will shift. In addition, in the presence of the plasma wave wiggler, there are four groups of orbits rather than just two, as found in the conventional wigglers (see figure 2).

Figure 4 shows the normalized total transverse magnetic field, $\mathbf{B}_{\rm trans.}[=(\mathbf{B}_{\rm sw}+\mathbf{B}_{\rm s})/\mathbf{B}_{\rm s}]$, as a function of the normalized cyclotron frequency, $\omega_{\rm c}$. As seen in this figure, for orbits of groups I and III, $\mathbf{B}_{\rm trans.}$ is higher than 1, therefore the wiggler-induced self-magnetic field, $\mathbf{B}_{\rm sw}$, is paramagnetic. On the other hand, for orbits of groups II and IV, $\mathbf{B}_{\rm trans.}$ is less than 1, meaning that the self-induced magnetic field is diamagnetic.

The graph of the normalized gain, $|G/G_0|$, where G_0 is G when $\omega_{\rm c} \to 0$, as a function of the normalized axial field frequency, $\omega_{\rm c}$, has been depicted in figure 5. As seen in this figure, on increasing the axial field frequency, the normalized gain for orbits of groups I and III increases monotonically to reach its maximum corresponding to the vicinity of the gyroresonance frequency. Whereas group II (and group IV) orbits start from $\omega_{\rm c} \approx 0.35$ (and $\omega_{\rm c} \approx 2$) and with increasing $\omega_{\rm c}$ the normalized gain decreases slowly. Similarly, the effect of $\omega_{\rm p}$ (or plasma density) on gain is shown in figures 6(a)–(d). As seen in these figures, with increasing normalized plasma frequency (or plasma density), orbits of groups I–IV shift to the right (i.e., to the higher cyclotron

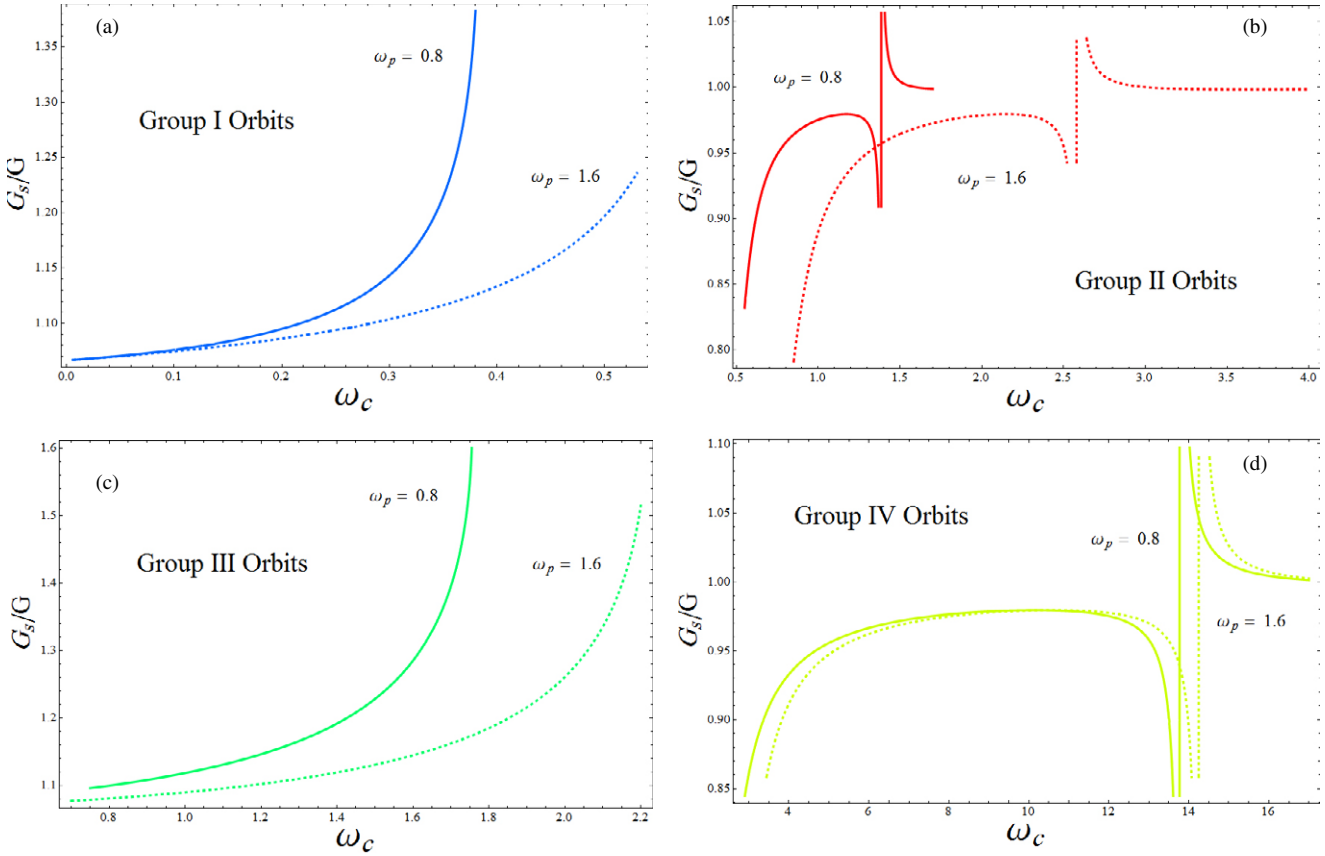

Figure 9. Graph of the gain ratio, $|G_{\rm self}/G|$, as a function of the normalized cyclotron frequency, $\omega_{\rm c}$, for $\omega_{\rm p} = 0.8$ and $\omega_{\rm p} = 1.6$ in orbits of (a) group I, (b) group II, (c) group III and (d) group IV. The chosen parameters are $\omega_{\rm b} = 0.08$, $\gamma = 200$ and $\Omega_{\rm s} = 0.07$.

frequencies). In figures 7(a)–(d), we show the effect of various γ on the gain. As seen in these figures, on varying γ from 40 to 200, the orbits of groups I–IV do not shift considerably.

Figure 8 shows the gain ratio $|G_{\rm self}/G|$ (i.e., the ratio of gain in the presence of self-fields to the gain in the absence of self-fields) as a function of the normalized cyclotron frequency, $\omega_{\rm c}$. As shown in this figure, the gain for orbits of groups I and III is greater than 1, so the effects of the beam self-fields causes gain enhancement. On the other hand, for orbits of groups II and IV, the gain ratio is less than 1, except near the critical point, therefore a decrease in gain is obtained due to the beam self-fields. The enhancement or decrease of the gain ratio are due to the paramagnetic or diamagnetic effects of the wiggler-induced self-magnetic field, respectively.

The effect of $\omega_{\rm p}$ (or plasma density) on the gain ratio, $|G_{\rm s}/G|$, is shown in figures 9(a)–(d). As seen in these figures, with increasing plasma frequency the orbits of all groups shift to the right, i.e., to higher cyclotron frequencies.

In summary, in this paper we have shown amplified emission in a FEL by a magnetized plasma medium. This gives rise to the possible reduction of the electron beam energy necessary to generate a shorter wavelength. The radiation can be confined by dielectric guiding in the plasma since the dielectric constant in the beam is larger than that of outside plasma due to the relativistic mass increase of its electron. Furthermore, this configuration has a higher tunability by controlling the plasma density in addition to the γ-tunability of the standard FEL.

Acknowledgment

This work was supported by the Science and Technology Research Center of Guilan University.

References

[1] Su J J, Katsouleas T, Dawson J M and Fedele R 1990 *Phys. Rev.* A **41** 3321
[2] Geddes C G R, Toth Cs, Van Tilborg J, Esarey E, Schroeder C B, Bruhwiler D, Nieter C, Cary J and Leemans W P 2004 *Nature* **431** 538
[3] Lambert G *et al* 2008 *Nature Phys.* **4** 296
[4] Freund H P, O'Shea P G and Biedron S G 2005 *Phys. Rev. Lett.* **94** 074802
[5] Piovella N, Cola M M, Volpe L, Schiavi A and Bonifacio R 2008 *Phys. Rev. Lett.* **100** 044801
[6] Bekefi G, Wurtele J S and Deutsch I H 1986 *Phys. Rev.* A **34** 1228
[7] Mehdian H, Jafari S and Hasanbeigi A 2011 *IEEE Trans. Plasma Sci.* **39** 761
[8] Sharma A and Tripathi V K 1996 *Phys. Plasmas* **3** 3116
[9] Kostyukov I, Kiselev S and Pukhov A 2003 *Phys. Plasmas* **10** 4818
[10] Esarey E, Shadwick B A, Catravas P and Leemans W P 2002 *Phys. Rev.* E **65** 056505
[11] Raghavi A and Mehdian H 2011 *Plasma Phys. Control. Fusion* **53** 105010
[12] McNeil B W J and Thomson N R 2010 *Nature Photon.* **4** 814
[13] Wang Z Y, Tang C J and Peng X D 2010 *Phys. Plasmas* **17** 083114
[14] Liu C S, Tripathi V K and Kumar N 2007 *Plasma Phys. Control. Fusion* **49** 325
[15] Whittum D H, Sessler A M and Dawson J M 1990 *Phys. Rev. Lett.* **64** 2511
[16] Chen K R and Dawson J M 1992 *Phys. Rev. Lett.* **68** 29
[17] Mehdian H and Raghavi A 2007 *Plasma Phys. Control. Fusion* **49** 69
[18] Whittum D H, Hiramatsu S and Kim J S 1993 *IEEE Trans. Plasma Sci.* **21** 170
[19] Petrillo V and Maroli C 2000 *Phys. Rev.* E **62** 8612
[20] Tsui K H, Serbeto A and D'olival J B 1998 *Phys. Rev.* E **57** 1029
[21] Andriyash I A, Humieres E D, Tikhonchuk T and Balcu Ph 2012 *Phys. Rev. Lett.* **109** 244802
[22] Tsui K H and Serbeto A 1998 *Phys. Rev.* E **58** 5013
[23] Pant K K and Tripathi V K 1994 *IEEE Trans. Plasma Sci.* **22** 217
[24] Qian B, Liu Y and Li C 1994 *Phys. Plasmas* **1** 4089
[25] Tripathi V K and Liu C S 1990 *IEEE Trans. Plasma Sci.* **18** 466
[26] Joshi C, Katsouleas T, Dawson J M, Yan Y T and Slater J M 1987 *IEEE J. Quantum Electron.* **23** 1571
[27] Sharma A and Tripathi V K 1993 *Phys. Fluids* B **5** 171
[28] Sharma A and Tripathi V K 1995 *IEEE Trans. Plasma Sci.* **23** 792
[29] Wen-Bing P and Ya-Shen C 1988 *Int. J. Electron.* **65** 551
[30] Kobayashi S, Antonsen T M and Nusinovich G S 1998 *IEEE Trans. Plasma Sci.* **26** 669
[31] Ganeev R A 2012 *Laser Phys. Lett.* **9** 175
[32] Agarwal R N and Tripathi V K 1995 *IEEE Trans. Plasma Sci.* **23** 788
[33] Freund H P and Antonsen J M 1996 *Principles of Free-electron Lasers* (London: Chapman and Hall)
[34] Kwan T and Dawson J M 1979 *Phys. Fluids* **22** 1089
[35] Mehdian H, Jafari S, Hasanbeigi A and Ebrahimi F 2009 *Nucl. Instrum. Methods Phys. Res.* A **604** 471
[36] Mehdian H, Jafari S and Hasanbeigi A 2010 *Plasma Phys. Control. Fusion* **52** 055005
Mehdian H, Jafari S and Hasanbeigi A 1995 *IEEE Trans. Plasma Sci.* **23** 792
[37] Yang Z, Chen H and Liang Z 2002 *Int. J. Infrared Millim. Waves* **23** 1057
[38] Kehs R A, Carmel Y and Granatstein V L 1990 *IEEE Trans. Plasma Sci.* **18** 437
[39] Freund H P, Kehs R A and Granatstein V L 1986 *Phys. Rev.* A **34** 2007
[40] Hafizi B and Roberson C W 1996 *Phys. Plasmas* **3** 2156
[41] Roberson C W and Sprangle P 1989 *Phys. Fluids* B **1** 3
[42] Chen K R and Dawson J M 1992 *Phys. Rev.* A **45** 4077
[43] Chen C and Davidson R C 1991 *Phys. Rev.* A **43** 5541
[44] Esmaeilzadeh M, Mehdian H, Willett J E and Aktas Y M 2003 *Phys. Plasmas* **10** 905
[45] Bourdier A and Michel L 1994 *Phys. Rev.* E **49** 3553
[46] Freund H P, Jackson R H and Pershing D E 1993 *Phys. Fluids* B **5** 2318
[47] Hafizi B and Roberson C W 1996 *Nucl. Instrum. Methods Phys. Res.* A **375** 78
[48] Hafizi B and Roberson C W 1992 *Phys. Rev. Lett.* **68** 3539
[49] Mirzanejhad S, Maraghechi B and Mohsenpour T 2004 *Phys. Plasmas* **11** 4777
[50] Mehdian H, Hasanbeigi A and Jafari S 2008 *Phys. Plasmas* **15** 123101
[51] Emma P, Huang Z, Kim K J and Pilot P 2006 *Phys. Rev. ST Accel. Beams* **9** 100702
[52] Wolski A, Penn G, Sessler A and Wurtele J 2004 *Phys. Rev. ST Accel. Beams* **7** 080701
[53] Zholents A A 2005 *Phys. Rev. ST Accel. Beams* **8** 050701

[54] Penn G, Sessler A and Wurtele J 2007 *Proc. PAC07 (Albuquerque, NM)* (Piscataway, NJ: IEEE) p 1176
[55] Stupakov G 2009 *Phys. Rev. Lett.* **102** 074801
[56] Rouhani M H and Maraghechi B 2010 *Phys. Rev. ST Accel. Beams* **13** 080706
[57] Freund H P, Nguyen D C and Carlsten B 2012 *Phys. Rev. ST Accel. Beams* **15** 030704
[58] Esmaeilzadeh M and Willett J E 2007 *Phys. Plasmas* **14** 033102
[59] Esmaeilzadeh M, Mehdian H and Willett J E 2002 *Phys. Rev.* E **65** 016501
[60] Freund H P and Gold S H 1984 *Phys. Rev. Lett.* **52** 926
[61] Freund H P, Davidson R C and Johnston G L 1990 *Phys. Fluids* B **2** 427
[62] Freund H P, Kehs R A and Granatstein V L 1985 *IEEE J. Quantum Electron.* **21** 1080
[63] Swanson D G 2003 *Plasma Waves* (Bristol: Institute of Physics Publishing)